Gümüşhane University Journal of Science

GUFBD / *GUJS* (2023) 13(1): 116-126 doi: 10.17714/gumusfenbil.1018705 Research Article

# Degradation evaluation of titanium dioxide under stress factors

*Titanyum dioksitin stres faktörleri altında bozunma değerlendirmesi*

**Ayşegül TAŞÇIOĞLU [1], Gökhan YILMAZ [*2]**

[1] *Burdur Mehmet Akif Ersoy University, Agriculture, Livestock and Food Research Application and Research Center, 15030, Burdur TURKEY*

[2] *Burdur Mehmet Akif Ersoy University, Faculty of Engineering and Architecture, Department of Energy System Engineering, 15030, Burdur, TURKEY*

• Received: 04.10.2022 • Accepted: 28.10.2022

**Abstract**

$TiO_2$ is used in many sectors of industry such as health, food, defense, and energy. It is a well-known fact that TiO2 is especially used in applications in the field of organic hybrid solar cells (OHSC) as an electron transfer layer in the energy sector. However, the OHSCs have a degradation problem because of atmospheric stress factors such as laboratory atmosphere, prolonged light application (light soaking), and UV light. To understand the meta/instability problem in OHSC, it is required to be examined independently for each layer consisting of the solar cell. In this study, the $TiO_2$ layer, widely used in OHSC applications, was grown on a rough glass substrate using a spin coating method. $TiO_2$ layer was structurally and electrically characterized by XRD and photoconductivity methods respectively. $TiO_2$ layer was characterized by exposure step by step to stress factors that are stated to cause electronic meta/instability in organic hybrid solar cells. Mobility-lifetime products were calculated from the flux-dependent photoconductivity and correlated with the electronic defects in the material due to stress factors. The findings in experiments show the laboratory atmosphere creates surface-related defects that can be eliminated by annealing. Light soaking, UV aging, and oxygen aging also create electronic defects associated with bandgap energy positions. These defects are partially eliminated with an annealing application.

**Keywords:** Electronic degradation, Mobility-lifetime product, Photoconductivity, Spin coating, Stress factors, Titanium dioxide.

***Öz***

*$TiO_2$ sağlık, gıda, savunma ve enerji gibi birçok sanayi sektöründe kullanılmaktadır. Özellikle organik hibrit güneş pilleri (OHGP) alanındaki uygulamalarda elektron transfer katmanı olarak kullanıldığı bilinmektedir. Ancak OHGP, laboratuvar atmosferi, ışıkta banyosu ve UV ışığı gibi dış stres faktörleri nedeniyle bozulma sorununa sahiptir. OHGP'de kısmi-kararsızlık/kararsızlık sorununun anlaşılabilmesi için hücreyi oluşturan her tabaka için ayrı ayrı incelenmesi gerekmektedir. Bu çalışmada, OHGP uygulamalarında yaygın olarak kullanılan $TiO_2$ tabakası pürüzlü cam taban malzeme üzerine Spin kaplama yöntemi ile büyütülmüştür. $TiO_2$ tabakası, sırasıyla XRD ve fotoiletkenlik yöntemi ile yapısal ve elektriksel olarak karakterize edilmiştir. $TiO_2$ tabakası, organik hibrit güneş pillerinde elektronik kısmi-kararsızlık/kararsızlık neden olduğu belirtilen stres faktörlerine birer birer maruz bırakılarak karakterize edilmiştir. Mobilite-yaşam süresi çarpımı, ışık akısına bağlı fotoiletkenlikten hesaplanmış ve stres faktörlerinden dolayı malzemedeki elektronik kusurlarla ilişkilendirilmiştir. Deneylerdeki bulgular, laboratuvar atmosferinin, tavlama ile ortadan kalkabilen yüzeyle ilgili kusurlar oluşturduğunu göstermektedir. Işık banyosu, UV yaşlanması ve oksijen yaşlanması da bant aralığı enerji konumlarıyla bağlantılı elektronik kusurlar yaratmaktadır. Tavlama uygulaması ile bu kusurlar kısmen ortadan kalkmaktadır.*

***Anahtar kelimeler**: Elektronik bozunma, Mobilite-yaşam süresi çarpımı, Fotoiletkenlik, Spin kaplama, Stres faktörleri, Titanyum dioksit.*

*Gökhan YILMAZ; gyilmaz@mehmetakif.edu.tr

## 1. Introduction

Perovskite solar cells (PSC), as a member of the organic hybrid solar cells family, especially methylammonium lead iodide ($MAPbI_3$) attract the attention of scientists with their high-efficiency characteristics among the solar cell family (Bhandarkar et al., 2021). However, it is known that there is remarkable degradation in the efficiency value of perovskite solar cells after a certain time following their production (Shaikh et al., 2017). This degradation in efficiency values is named as instability or metastability (Kim et al., 2012; Lee et al., 2012). There are various reasons for this efficiency degradation in perovskite solar cells (Green et al., 2014). A few of these can be defined as layer degradation, interface interactions, and ongoing chemical reactions due to solution-based production of the layers that make up the solar cell. (Prathvi et al., 2021; Zhou et al., 2014). In the literature, environmental stress factors such as water vapor, UV light, oxygen, and light soaking are defined as the most prominent stress factors (Leijtens et al., 2013). To understand this instability in perovskite solar cells, each layer of the solar cell must be produced independently and the degradation of the layers by exposure to different stress factors one by one must be understood (Christians et al., 2015).

The first layer of perovskite solar cells is the electron transfer layer (ETL). In the literature, there are many ETL candidates for perovskite solar cells. Electron transport layers should have some specifications such as (i) ETLs should have high transparency, (ii)ETLs should have well-matched energy alignment with the absorber layer, and (iii)ETLs should have high electron mobility (Akin et al., 2020; Shalan et al., 2020; Zaki et al., 2020). Depending on these parameters the most promising candidates are $TiO_2$, SnO2, ZnO, Zn,2SnO4, and WO3 as ETLs. Among them, the preferred ETLs are $TiO_2$, ZnO, and SnO2. Among these candidates, TiO2 is the most used ETLs in PSC, especially in the most highly- efficient PSC including the current -record holder. However, each candidate has advantages and disadvantages. For example, ZnO creates a degradation of perovskite solar cells. Methylammonium cations in the perovskite film of solar cells are destroyed by ZnO. (Cao et al., 2018; Aslan et al., 2016; Azmi et al., 2018; Goktas et al., 2019; Song et al., 2016a, b; Tumbul et al., 2019). In the same way, SnO2 thin-film production needed high-temperature processes which also ruin the perovskite structure. On the other hand, the unit price of SnO2 is much more than TiO2. For example, 100g (%99) TiO2 is 407€ and 5g (%99) SnO2 is 241€. This situation indicates that the industrial application of SnO2 is not commercially available. It is clearly understood that the most preferred ETL is TiO2 for efficiency and price. In addition to all, Titanium dioxide (TiO2) has many interesting physical properties such as good transmittance in the visible region, high refractive index, high dielectric constant, and chemical stability which make TiO2 thin films suitable for in microelectronic devices, capacitors, or as a gate dielectric in metal-dielectric-semiconductor devices (Yoldas et al., 1979; Yoldas 1982; Fuyuki et al., 1986; Bertrand et al., 1983). There are several techniques have been used to prepare TiO2 thin films, such as sputtering (Schiller et al., 1981; Suhail et al., 1992; Okimura et al., 1996), chemical vapor deposition (CVD) (Yeung et al., 1983 ; Lu et al., 1991), thermal oxidation (Burns, 1989), pyrolysis (Rice, 1987; Zhang et al. 1992) and sol-gel ( Yoko et al., 1991; Vorotilov et al., 1992; Nagpal et al.,1995).

In this study, the $TiO_2$ layer used in the organic hybrid solar cell was grown on a rough glass substrate with the spin coating method and exposed to stress factors (laboratory atmosphere, light soaking, UV aging, and high-purity oxygen gas). Structural characterizations were done with XRD, SEM, and EDS. Electrical characterizations such as photoconductivity were done to understand the changes in the material by atmospheric effect.

## 2. Material and method

$TiO_2$ materials were grown with a solution process by spin coating. 5 ml ethanol solution was prepared with 1.4 grams of titanium isopropoxide (Sigma Aldrich %99.7). Since titanium isopropoxide is a volatile substance, ethanol was poured directly onto titanium isopropoxide in an ice bath. The resulting solution was coated with a spin coating system rotating at 1300 rpm by dropping 5 ml onto the substrate material. The coated films were left to dry on the heating surface at 80 °C for half an hour to remove the volatiles from the $TiO_2$ film. After the production of $TiO_2$ film, the post-annealing procedure was applied at 500°C. To control structural features of $TiO_2$, XRD, and SEM, EDS measurements were done. XRD measurements were done by Bruker AXS D8 advanced measuring system and a Cu tube was used for the X-ray source. Measurements were carried out in the 2 theta range from 10 to 80 degrees and are shown in figure 1. Scanning Electron Microscopy (SEM) and Energy Dispersive Spectroscopy (EDS) measurements were done by FEI Quanta FEG 250, under low vacuum (60 Pa) and High Voltage 20.00kV with 20.000 magnification. Silver metal contacts

were grown on the TiO2 films with the thermal evaporation method for conductivity measurements. The coplanar contact geometry was applied to the $TiO_2$ films, with a thickness of $5.0x10^{-9}$ m, contact lengths of $5.0x10^{-3}$ m, and contact distance between contacts of $5.0x10^{-4}$ m.

To explain a measurement procedure, one full cycle of measurement was tried to be summarized below. $TiO_2$ thin film was placed in the cryostat in the laboratory atmosphere and the Ohmic voltage was determined by I-V measurement. By applying the determined Ohmic voltage, time-dependent dark conductivity values were started to be recorded in the cryostat in the dark environment. When the dark conductivity values became stable, a photoconductivity measurement was carried out depending on the flux. Then, the system was placed under a vacuum and when the dark conductivity values became stable, the photoconductivity values were taken again in the vacuum atmosphere depending on the flux. After that, the material was heated up to 450K with a temperature increase of 2K per minute without disturbing the vacuum environment, and after being exposed to heat treatment at 450K for 30 minutes, it was cooled to 300K by a 2K ramp. While the dark conductivity values were stable at 300K in the vacuum environment, the photoconductivity measurement was carried out depending on the flux in the annealed-1 state of the material. These steps were repeated in each stress factor (laboratory atmosphere, light soaking, UV aging, and oxygen aging). After each stress factor application, the photoconductivity values of the material were measured depending on the flux in conditions where the material was stable. Depending on the flux that is applied, the generation rate was calculated (Yılmaz, 2021). In addition to this, by using photoconductivity values that are obtained, the mobility-lifetime of the material was calculated (Yılmaz, 2021). By using these two calculated data, the graphs of the mobility-life time vs. generation rate of the $TiO_2$ material were drawn and interpretations could be made about the electronic defect changes in the material from the behavior of these graphs. These graphs have given the chance of understanding defect density and defect types variance depending on previous conditions.

## 3. Results

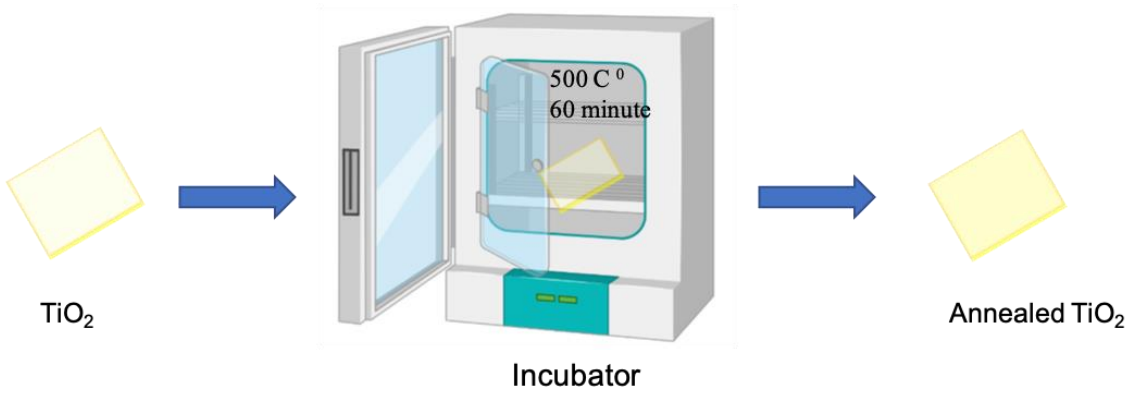


**Figure 1**. $TiO_2$ thin film post-annealing procedure

As seen in figure 2; XRD data shows that after post-annealing on $TiO_2$ film was established by anatase phase and this situation is seen consistent with the previous data in the literature. In addition, XRD peaks were indexed from the "Joint Committee on Powder Diffraction Standards (JCPDS)" database with the card number 00-004-0477 (Jalali et al., 2020; Sun et al., 2015). Detailed structural analysis (SEM and EDS measurements) were also carried out on $TiO_2$ thin films. In figure 3 SEM images and EDS results of post-annealed and as-deposited $TiO_2$ were displayed.

As clearly seen from figure 3a, after post-annealing $TiO_2$ film structure gets much more porous than the as-grown structure in figure 3b. Post annealing create porosity and increase the inner surface area of $TiO_2$ thin films. This result match with the previous data in the literature (Kim et al., 2007; Haidry et al., 2012; Wang et al., 2015). In addition that, the EDS results in figure 3c, show that there are only titanium and oxygen elements consisting of a thin film structure.

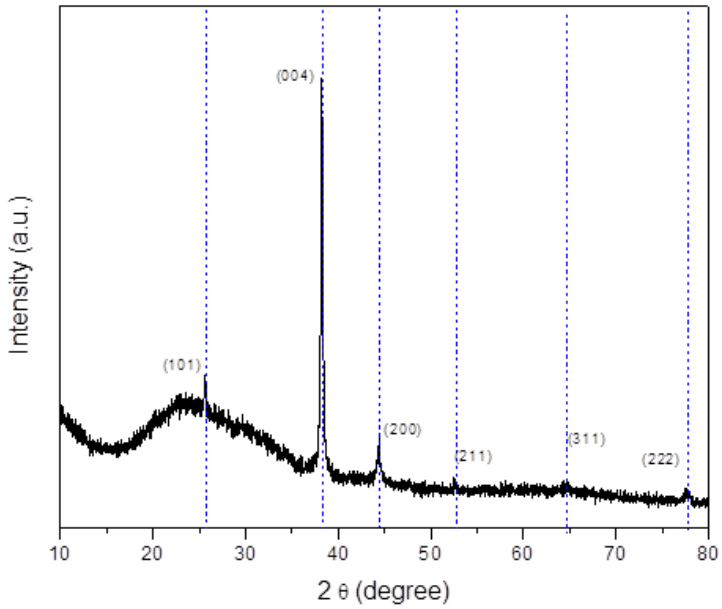


**Figure 2**. XRD analysis of $TiO_2$ thin film

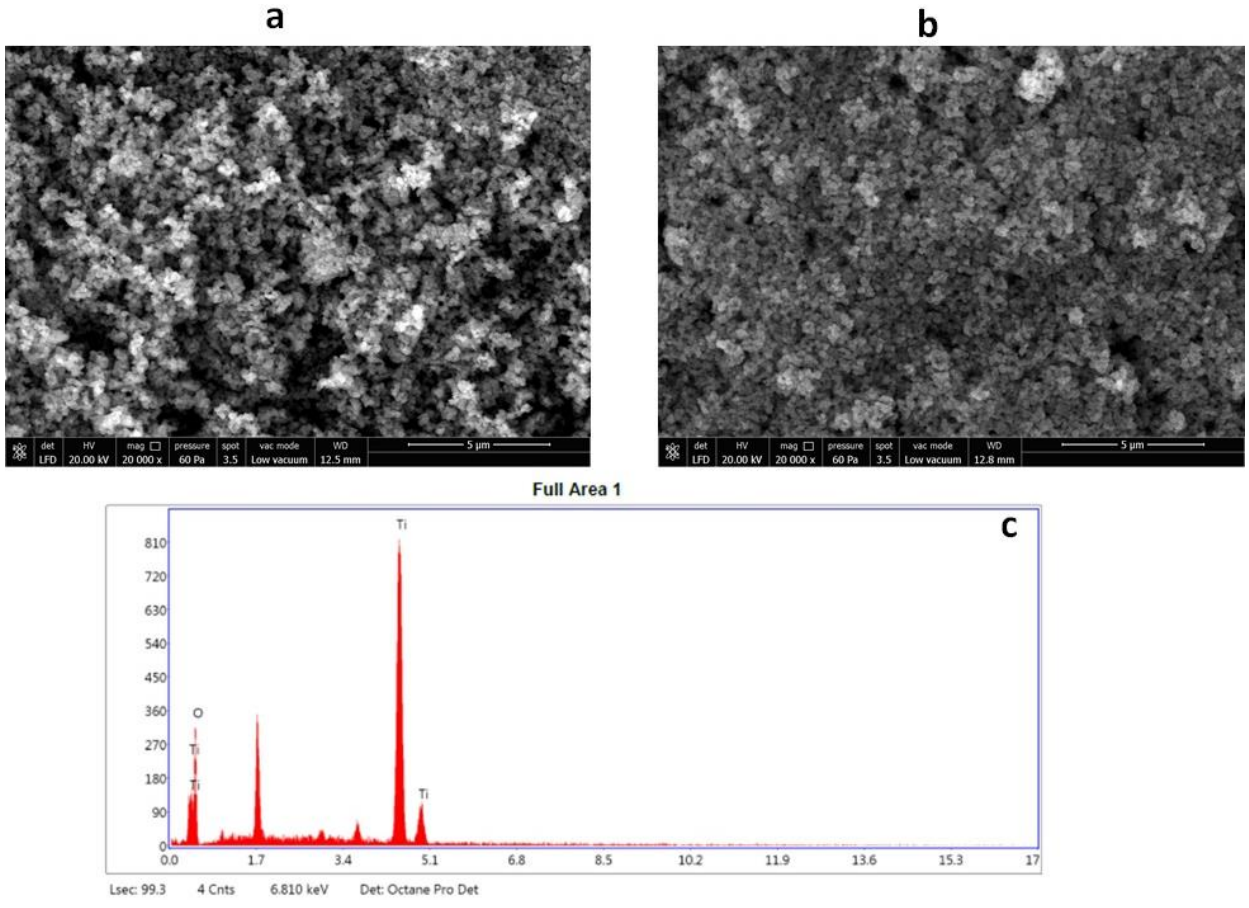


**Figure 3**. SEM and EDS analysis of $TiO_2$ thin film (a) post annealed $TiO_2$ thin film with 20.000 magnification SEM image, (b) as-deposited $TiO_2$ thin film with 20.000 magnification SEM image, (c) post annealed $TiO_2$ thin film EDS results.

Figure 4a shows the photoconductivity values obtained after laboratory atmosphere, vacuum atmosphere, and annealed-1 state. As can be seen in figure 4a, the photoconductivity values obtained in the laboratory atmosphere and the vacuum atmosphere overlaps. However, with annealed-1, a significant decrease (approximately 7-times decrease) was observed in photoconductivity values, especially in the medium and

high flux ($10^{16}$ – $10^{17}$ $cm^{-2}$ $s^{-1}$) region. The main reason for the decrease in photoconductivity values after heat treatment, may be due to the atmospheric gas molecules that could be attached to the surface of the thin film. The gas molecules attached to the surface may have been removed from the surface with the effect of vacuum and heat treatment. As a result, a change in the photoconductivity values of the material may have taken place.

In figure 4b, the photoconductivity values of the material after annealed-1 and after annealed -2 stages, were compared after 30 minutes of exposure to five sun intensities of light (5x A.M.1.5). In figure 4b, it is seen that there is a 1.5 times decrease in photoconductivity values due to the light soaking applied to the material after the annealed-1 application. In addition, an increase in the slope of the photoconductivity values is observed after the light soaking in the high flux region. In literature, the same degradation was also observed in perovskite solar cell structure (Chong et al., 2020). This may be due to an increase in the electronic defect states of the material after the light soaking. This increase in electronic defect state changes directly affects the photoconductivity values. It was determined that the behavior or type change of the electronic defect, especially in the high flux ($10^{17}$ $cm^{-2}$ $s^{-1}$) region, increased photoconductivity values in figure 4b. After the second heat treatment was carried out, the photoconductivity values exceeded the annealed-1 values and exhibited an increase of approximately two times compared to the values in the light soaking.

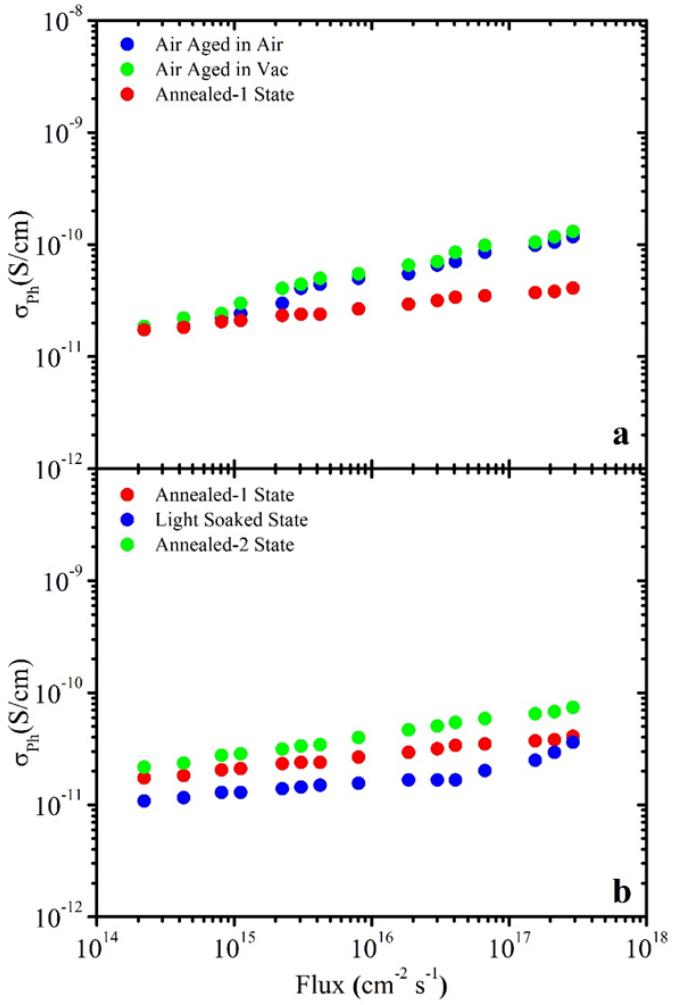


**Figure 4.** $TiO_2$ thin film flux dependent photoconductivity results; (a) air aged state and annealed state-1 (b) light-soaked state and annealed states 1-2

When the UV aging literature studies are examined on TiO2, it is seen that TiO2 material is generally used as a coating that prevents UV aging (Zang et al., 2017; Sun et al., 2011). On the other hand, any information about the electronic degradation of TiO2 itself due to UV aging was not realized. In figure 5a, 30 minutes of UV light was applied to the material and the photoconductivity values were recorded after UV aging. As can be seen in figure 5a, the photoconductivity values also decreased below the photoconductivity values in the light soaking. In addition, the slope change seen in figure 4b, at high flux values, began to be seen at medium

flux ($10^{15}$ – $10^{16}$ $cm^{-2}$ $s^{-1}$) intensities. Although similar behavior was observed after light soaking, it was determined that this behavior was much more significant after UV aging. At the same time, the slope change which was observed at the high flux ($10^{17}$ $cm^{-2}$ $s^{-1}$) region after the light soaking, starts from the medium flux ($10^{16}$ $cm^{-2}$ $s^{-1}$) region at this time. However, these slope changes disappear with the annealed-3 application and the photoconductivity values approach the annealed-2 values.

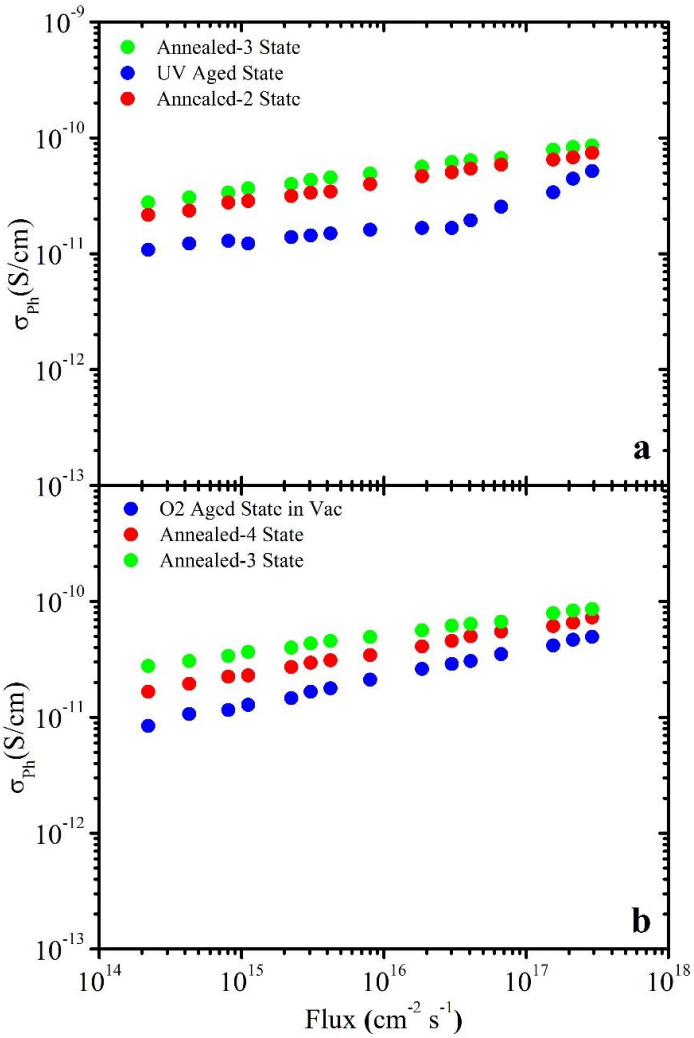


**Figure 5**. $TiO_2$ thin film flux dependent photoconductivity results (a) UV aged state and annealed states 2-3 (b) oxygen aged state and annealed states 3-4.

In figure 5b, the photoconductivity change, obtained in a vacuum atmosphere after the application of high-purity oxygen gas to the system, is presented. In the literature, any information about aging TiO2 by exposure to oxygen gas after production could not be reached. However, it has been reported that, oxygen gas is sent to the system during TiO2 production. Thus, this application enlarges the grain structures during the production and accordingly causes an increase in the conductivity (Duran et al., 2019). In figure 5b, photoconductivity values decreased sharply after oxygen gas application. This reduction is approximately seven times greater while compared to the annealed-3 condition. Although it contains a high percentage of oxygen in the $TiO_2$ film structure, it is very interesting to see the decrease in photoconductivity values with the application of oxygen gas. There may be three main reasons for this situation. The first reason could be the fact that, oxygen is physically attached to the surface and changed conductivity. The second is that, the oxygen makes bonds with the open structures (dangling bonds) on the surface, and the third is that it occurs together in both cases described above. Although the photoconductivity values increased approximately five times with the stage annealed-4, conductivity values could not reach the annealed-3 state. This situation displays that, the oxygen application creates a partially reversible effect on $TiO_2$ film.

In figure 6, after applying each different stress factor to the $TiO_2$ film, the graph of generation rate versus the mobility-lifetime product is presented. Mobility-lifetime calculation and generation rate calculation can be found in detail in previous studies (Yılmaz, 2021). As can be seen in figure 6a, the light soaking application was applied to the material after the annealed-1 state and it was determined that there was two-times decrease in the mobility-lifetime products. This display that, the light soaking increases the electronic defect density in the bandgap of the material. Thus, mobility-lifetime product decreases significantly. This increase in the electronic defect density completely disappears with the second annealing application and even it exceeded the values obtained in the annealed-1 state. In this case, it can be said, the electronic defects, consisting of the material after the light soaking with the second annealing application, are eliminated and the electronic defect type and density of the material change.

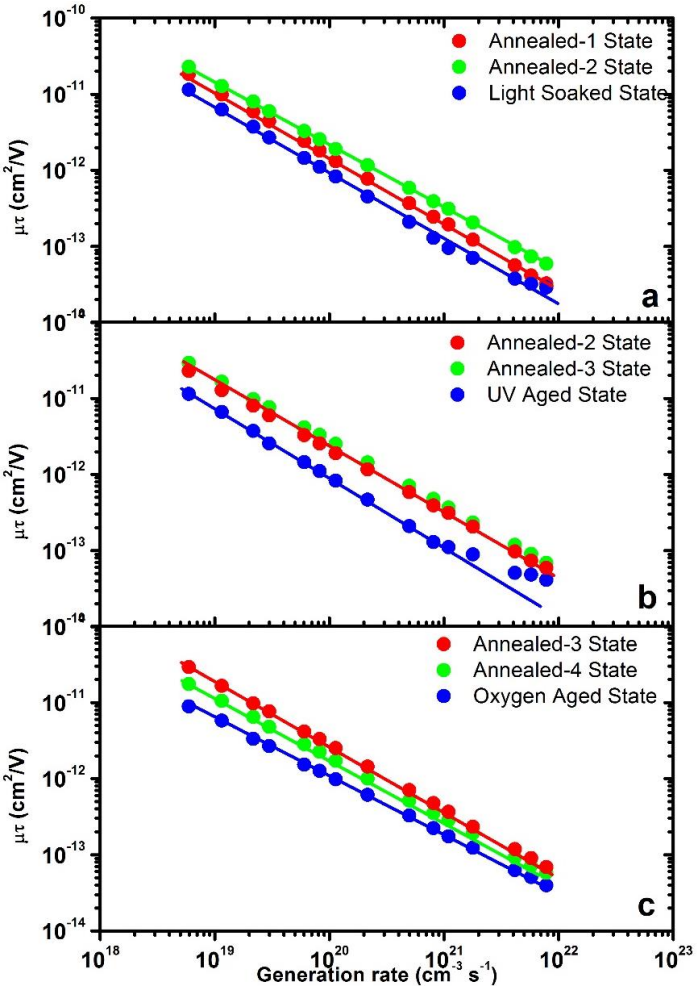


**Figure 6.** $TiO_2$ thin film mobility-lifetime dependent generation rates; (a) light-soaked state and annealed states 1-2 (b) UV aged state and annealed states 2-3 (c) oxygen aged state and annealed state 3-4

In figure 6b, UV aging was performed after the second annealing application of the material, and it was observed that there was two-times decrease in the mobility lifetime products. In addition, it was determined that the mobility-lifetime slope also changed in the region of a high generation rate ($10^{21}$ $cm^{-3}$ $s^{-1}$). This shows that different types of electronic defects could be occurred in the regions close to the conduction band due to UV aging. After the third annealing, the mobility-lifetime product values reach the values obtained in the annealed-2 state. This situation shows us that the electronic defect types created in the material by UV aging are completely reversible with heat treatment.

In figure 6c, the values obtained as a result of the mobility-lifetime product after high purity oxygen gas, is applied to the material is displayed. Mobility-lifetime values of the material with the oxygen gas application show a sharp decrease of approximately four times in the region of low generation rate ($10^{18}$ $cm^{-3}$ $s^{-1}$). At high generation rates, this rate drops to 1.5 times. The fourth annealing values show that, mobility-lifetime product

values partially approximately reach the annealed-3 state results. This shows that oxygen gas significantly changes the electronic defect density of the material, and it creates a partially reversible effect on the material.

## 4. Conclusions

In this study, $TiO_2$ thin film, that is frequently used in organic solar cells as an electron transfer layer, was produced with the spin coating method, and electronic defect changes with the application of a single stress factor were examined in detail by the photoconductivity method. In light of findings, it was determined that the light soaking caused a significant increase in the electronic defect density of the $TiO_2$ material, but this increase was eliminated with the annealing procedure. Similarly, UV light creates an apparent electronic defect increase in $TiO_2$ film. It was also determined that there were changes in the electronic defect types at the high generation rate region because of UV aging. However, these changes in defect density and types are eliminated by annealing. It was determined that there was an increase in the electronic defect density in the $TiO_2$ film material with the application of oxygen gas, but this increase did not completely reversible with the application of annealing, and it created a partial reversible effect. The reason for this change in the oxygen gas, may have been the chemical bonding between the open bonds in the $TiO_2$ structure and the oxygen molecules.

## Acknowledgments

The authors would like to thank Dr. Friedhelm FINGER and Julich Research Center Germany for their donations. The authors also would like to thank the editors and referees for their contributions during the review and evaluation process of the article.

## Author contribution

The authors have equal contribution to the formation of this article.

## Declaration of ethical code

The authors of this article declare that materials and methods used in this study do not require ethical committee approval and/or legal-specific permission.

## Conflicts of interest

The authors declare that there is no conflict of interest.

## References

Akin, S., Akman, E., & Sonmezoglu, S. (2020). FAPbI3- based Perovskite solar cells employing hexyl-based ionic liquid with an efficiency over 20% and excellent long-term stability. *Adv Funct Mater.* https://doi.org/10.1002/adfm.20200 2964.

Aslan, F., Tumbul, A., Göktaş, A., Budakoğlu, R., & Mutlu, İ. H. (2016). Growth of ZnO nanorod arrays by one-step sol-gel process. *Journal of Sol-Gel Science and Technology*, *80*(2), 389-395. https://doi.org/10.1007/s10971-016-4131-z

Azmi, R., Hadmojo, W. T., Sinaga, S., Lee, C. L., Yoon, S. C., Jung, I. H., & Jang, S. Y. (2018). High-efficiency low-temperature ZnO based perovskite solar cells based on highly polar, nonwetting self-assembled molecular layers. *Advanced Energy Materials*, *8*(5), 1701683. https://doi.org/10.1002/aenm.201701683

Baranowska-Wójcik, E., Szwajgier, D., Oleszczuk, P., & Winiarska-Mieczan, A. (2020). Effects of titanium dioxide nanoparticles exposure on human health—a review. *Biological Trace Element Research*, *193*(1), 118-129. https://doi.org/10.1007/s12011-019-01706-6

Bertrand, P. A., & Fleischauer, P. D. (1983). Chemical deposition of TiO2 layers on GaAs. *Thin Solid Films*, *103*(1-3), 167-175. https://doi.org/10.1016/0040-6090(83)90433-9

Bhandarkar, S. A., Kompa, A., Murari, M. S., Kekuda, D., & Mohan, R. K. (2021). Investigation of structural and optical properties of spin coated TiO2: Mn thin films. *Optical Materials*, *118*, 111254.

https://doi.org/10.1016/j.optmat.2021.111254

Burns, G. P. (1989). Titanium dioxide dielectric films formed by rapid thermal oxidation. *Journal of applied physics*, *65*(5), 2095-2097. https://doi.org/10.1063/1.342856

Cao, J., Wu, B., Chen, R., Wu, Y., Hui, Y., Mao, B. W., & Zheng, N. (2018). Efficient, hysteresis-free, and stable perovskite solar cells with ZnO as electron-transport layer: effect of surface passivation. *Advanced Materials*, *30*(11), 1705596. https://doi.org/10.1002/adma.201705596

Castro-Chong, A., Qiu, W., Bastos, J., Yimga, N. T., García-Rodríguez, R., Idígoras, J., Anta, J. A., Aernouts, T., & Oskam, G. (2020). Impact of the implementation of a mesoscopic TiO2 film from a low-temperature method on the performance and degradation of hybrid perovskite solar cells. *Solar Energy*, *201*, 836-845. https://doi.org/10.1016/j.solener.2020.03.041

Christians, J. A., Manser, J. S., & Kamat, P. V. (2015). Best practices in perovskite solar cell efficiency measurements. Avoiding the error of making bad cells look good. *The journal of physical chemistry letters*, *6*(5), 852-857. https://doi.org/10.1021/acs.jpclett.5b00289

Dorier, M., Béal, D., Marie-Desvergne, C., Dubosson, M., Barreau, F., Houdeau, E., Herlin-Boime, N., & Carriere, M. (2017). Continuous in vitro exposure of intestinal epithelial cells to E171 food additive causes oxidative stress, inducing oxidation of DNA bases but no endoplasmic reticulum stress. *Nanotoxicology*, *11*(6), 751-761. https://doi.org/10.1080/17435390.2017.1349203

Dundar, I., Krichevskaya, M., Katerski, A., & Acik, I. O. (2019). TiO2 thin films by ultrasonic spray pyrolysis as photocatalytic material for air purification. *Royal Society open science*, *6*(2), 181578. https://doi.org/10.1098/rsos.181578

El-Henawey, M. I., Kubas, M., El-Shaer, A., & Salim, E. (2021). The effect of post-annealing treatment on the structural and optoelectronic properties of solution-processed TiO2 thin films. *Journal of Materials Science: Materials in Electronics*, *32*(16), 21308-21317. https://doi.org/10.1007/s10854-021-06633-8

Fuyuki, T., & Matsunami, H. (1986). Electronic properties of the interface between Si and TiO2 deposited at very low temperatures. *Japanese Journal of Applied Physics*, *25*(9R), 1288. https://dx.doi.org/10.1143/JJAP.25.1288

Goktas, A., Tumbul, A., Aba, Z., & Durgun, M. (2019). Mg doping levels and annealing temperature induced structural, optical and electrical properties of highly c-axis oriented ZnO: Mg thin films and Al/ZnO: Mg/p-Si/Al heterojunction diode. *Thin Solid Films*, *680*, 20-30. https://doi.org/10.1016/j.tsf.2019.04.024

Green, M. A., Ho-Baillie, A., & Snaith, H. J. (2014). The emergence of perovskite solar cells. *Nature photonics*, *8*(7), 506-514. https://doi.org/10.1038/NPHOTON.2014.134

Jalali, E., Maghsoudi, S., & Noroozian, E. (2020). A novel method for biosynthesis of different polymorphs of TiO2 nanoparticles as a protector for Bacillus thuringiensis from Ultra Violet. *Scientific Reports*, *10*(1), 1-9. https://doi.org/10.1038/s41598-019-57407-6

Kim, H. S., Lee, C. R., Im, J. H., Lee, K. B., Moehl, T., Marchioro, A., Moon, S.J., Humphry-Baker, R., Yum, J., Moser, J.E., Gra¨tzel, M., & Park, N.G. (2012). Lead iodide perovskite sensitized all-solid-state submicron thin film mesoscopic solar cell with efficiency exceeding 9%. *Scientific reports*, *2*(1), 1-7. https://doi.org/10.1038/srep00591

Lee, M. M., Teuscher, J., Miyasaka, T., Murakami, T. N., & Snaith, H. J. (2012). Efficient hybrid solar cells based on meso-superstructured organometal halide perovskites. *Science*, *338*(6107), 643-647. https://doi.org/10.1126/science.1228604

Leijtens, T., Eperon, G. E., Pathak, S., Abate, A., Lee, M. M., & Snaith, H. J. (2013). Overcoming ultraviolet light instability of sensitized TiO2 with meso-superstructured organometal tri-halide perovskite solar cells. *Nature communications*, *4*(1), 1-8. https://doi.org/10.1038/ncomms3885

Lu, J. P., Wang, J., & Raj, R. (1991). Solution precursor chemical vapor deposition of titanium oxide thin films. *Thin Solid Films*, *204*(1), L13-L17. https://doi.org/10.1016/0040-6090(91)90488-J

Nagpal, V. J., Davis, R. M., & Desu, S. B. (1995). Novel thin films of titanium dioxide particles synthesized by a sol-gel process. *Journal of materials research*, *10*(12), 3068-3078. https://doi.org/10.1557/JMR.1995.3068

Okimura, K., Maeda, N., & Shibata, A. (1996). Characteristics of rutile TiO2 films prepared by rf magnetron sputtering at a low temperature. *Thin solid films*, *281*, 427-430. https://doi.org/10.1016/0040-6090(96)08659-2

Rice, G. W. (1987). Laser-Driven Pyrolysis: Synthesis of TiO2 from Titanium Isopropoxide. *Journal of the American Ceramic Society*, *70*(5), C-117. https://doi.org/10.1111/j.1151-2916.1987.tb05020.x

Schiller, S., Beister, G., Sieber, W., Schirmer, G., & Hacker, E. (1981). Influence of deposition parameters on the optical and structural properties of TiO/sub 2/films produced by reactive dc plasmatron sputtering. *Thin Solid Films;(Switzerland)*, *83*(2). https://doi.org/10.1016/0040-6090(81)90673-8

Shaikh, J. S., Shaikh, N. S., Sheikh, A. D., Mali, S. S., Kale, A. J., Kanjanaboos, P., Hong, J.K., Kim, J.H., & Patil, P. S. (2017). Perovskite solar cells: In pursuit of efficiency and stability. *Materials & Design*, *136*, 54-80. https://doi.org/10.1016/j.matdes.2017.09.037

Shalan, A. E. (2020). Challenges and approaches towards upscaling the assembly of hybrid perovskite solar cells. *Materials Advances*, *1*(3), 292-309. https://doi.org/10.1039/D0MA00128G

Simionescu, O. G., Romanițan, C., Tutunaru, O., Ion, V., Buiu, O., & Avram, A. (2019). RF magnetron sputtering deposition of TiO2 thin films in a small continuous oxygen flow rate. *Coatings*, *9*(7), 442. https://doi.org/10.3390/coatings9070442

Song, J., Zheng, E., Liu, L., Wang, X. F., Chen, G., Tian, W., & Miyasaka, T. (2016a). Magnesium-doped Zinc Oxide as Electron Selective Contact Layers for Efficient Perovskite Solar Cells. *ChemSusChem*, *9*(18), 2640-2647. https://doi.org/10.1002/cssc.201600860

Song, J., Hu, W., Wang, X. F., Chen, G., Tian, W., & Miyasaka, T. (2016b). HC(NH 2)2PbI3 as a thermally stable absorber for efficient ZnO-based perovskite solar cells. Journal of Materials Chemistry A, 4(21), 8435-8443.https://doi.org/10.1039/C6TA0 1074A

Suhail, M. H., Rao, G. M., & Mohan, S. D. C. J. (1992). dc reactive magnetron sputtering of titanium-structural and optical characterization of TiO2 films. Journal of Applied Physics, 71(3), 1421-1427. https://doi.org/10.1063/1.351264

Sun, S. S., Wang, Y. M., & Zhang, A. Q. (2011). Study on anti-ultraviolet radiation aging property of TiO2 modified asphalt. In *Advanced materials research* , 306, (951-955). https://doi.org/10.4028/www.scientific.net/AMR.306-307.951

Sun, H., Peng, T., Liu, B., & Xian, H. (2015). Effects of montmorillonite on phase transition and size of TiO2 nanoparticles in TiO2/montmorillonite nanocomposites. *Applied Clay Science*, *114*, (440-446). https://doi.org/10.1016/j.clay.2015.06.026

Tumbul, A., Aslan, F., Demirozu, S., Goktas, A., Kilic, A., Durgun, M., & Zarbali, M. Z. (2018). Solution processed boron doped ZnO thin films: influence of different boron complexes. *Materials Research Express*, *6*(3), 035903. https ://doi.org/10.1088/2053-1591/aaf4d 8

Vorotilov, K. A., Orlova, E. V., & Petrovsky, V. I. (1992). Sol-gel TiO2 films on silicon substrates. *Thin Solid Films*, *207*(1-2), 180-184. https://doi.org/10.1016/0040-6090(92)90120-Z

Yeung, K. S., & Lam, Y. W. (1983). A simple chemical vapour deposition method for depositing thin TiO2 films. *Thin Solid Films*, *109*(2), 169-178. https://doi.org/10.1016/0040-6090(83)90136-0

Yılmaz, G. 2021. Creation and Investigation of Electronic Defects on Methylammonium Lead Iodide (CH3NH3PbI3) Films Depending on Atmospheric Conditions. *European Physical Journal D 75*(6). https://doi.org/10.1140/epjd/s10053-021-00167-8

Yoko, T., Yuasa, A., Kamiya, K., & Sakka, S. (1991). Sol-gel-derived TiO2 film semiconductor electrode for photocleavage of water: preparation and effects of post heating treatment on the photoelectrochemical behavior. *Journal of the Electrochemical Society*, *138*(8), 2279. https://doi.org/10.1149/1.2085961

Yoldas, B. E., & O'Keeffe, T. W. (1979). Antireflective coatings applied from metal–organic derived liquid precursors. *Applied Optics*, *18*(18), 3133-3138.https://doi.org/10.1364/AO.18.003133

Yoldas, B. E. (1982). Deposition and properties of optical oxide coatings from polymerized solutions. *Applied Optics*, *21*(16), 2960-2964. https://doi.org/10.1364/AO.21.002960

Zaki, A. H., Shalan, A. E., El-Shafeay, A., Gadelhak, Y. M., Ahmed, E., Abdel-Salam, M. O., Sobhi, M., & El-dek, S. I. (2020). Acceleration of ammonium phosphate hydrolysis using TiO2 microspheres as a catalyst for hydrogen production. *Nanoscale Advances, 2*(5), 2080-2086. https://doi.org/10.1039/D0NA00204F

Zhang, S. Y. F. D. E., Zhu, Y. F., & Brodie, D. E. (1992). Photoconducting TiO2 prepared by spray pyrolysis using TiCl4. *Thin Solid Films, 213*(2), 265-270. https://doi.org/10.1016/0040-6090(92)90292-J

Zhang, H., Yang, H., Shentu, B., Chen, S., & Chen, M. (2018). Effect of titanium dioxide on the UV‐C ageing behavior of silicone rubber. *Journal of Applied Polymer Science, 135*(14), 46099. https://doi.org/10.1002/app.46099

Zhou, H., Shi, Y., Dong, Q., Zhang, H., Xing, Y., Wang, K., Du, Y., & Ma, T. (2014). Hole-conductor-free, metal-electrode-free TiO2/CH3NH3PbI3 heterojunction solar cells based on a low-temperature carbon electrode. *The journal of physical chemistry letters, 5*(18), 3241-3246. https://doi.org/10.1021/jz5017069